Quantum breathing mode of trapped bosons and fermions at arbitrary coupling

S. Bauch, K. Balzer, C. Henning, and M. Bonitz[*]

Institut für Theoretische Physik und Astrophysik, Christian-Albrechts-Universität zu Kiel, D-24098 Kiel, Germany

Interacting particles in a harmonic trap are known to possess a radial collective oscillation—the breathing mode (BM). We show that a quantum system has *two* BMs and analyze their properties by exactly solving the time-dependent Schrödinger equation. We report that the frequency of one BM changes with system dimensionality, the particle spin and the strength of the pair interaction and propose a scheme that gives direct access to key properties of trapped particles, including their many-body effects.

PACS number(s): 67.85.−d, 03.75.Kk, 03.75.Ss, 05.30.−d

I. INTRODUCTION

The dynamics of trapped quantum systems are of growing interest in many fields, including correlated electrons in metal clusters[1] or quantum dots[2–4] and ultracold Bose and Fermi gases in traps or optical lattices, for recent overviews see, e.g.,[5,6] Particular attention has recently been devoted to Bose-Einstein condensation in low dimensions[7] and to the analysis of nonideality (interaction) effects,[8–11] including superfluidity and crystallization, see Ref. 12. At the same time, nonideal low-dimensional Bose and Fermi systems present major experimental and theoretical challenges. For a reliable diagnostics of static and time-dependent properties, the collective oscillations of the system play a key role.[6,8,9] It is the purpose of this paper to show that, among them, the monopole or breathing mode (BM) which is easily excited experimentally[8] carries particularly valuable information on the system dimensionality d, the spin statistics of the particles and on the form and relative strength λ of their pair interaction given by Eqs. (2) and (3).

The BM of a system of N particles in a harmonic trap with frequency Ω is well known in two limiting cases: in the limit of very strong interparticle repulsion ($\lambda \to \infty$) with an inverse power-law potential, $w(|\mathbf{r}|) \sim r^{-l}$, the particles behave classically being spatially localized, and the BM which describes the radial expansion/contraction of a cloud of well-separated particles is independent of N and d,[13,14] whereas its frequency is sensitive to the interaction, $\omega_{BM} = \sqrt{2l+1}\ \Omega$. In the second limiting case, that of an ideal quantum gas with $\lambda = 0$, the BM corresponds to a periodic expansion/contraction of the wave function with frequency $\omega_{BM} = 2\Omega$, which is, of course, independent of N, d, and the type of the interaction, see Sec. III A.

This raises the question about ω_{BM} for *arbitrary finite values of the interaction strength* which we answer in this paper. While our results for the BM are representative for any nonideal quantum system in a harmonic trap, here, we concentrate on a complete analysis of the case of Coulomb interaction ($l=1$). We present exact numerical results from solutions of the time-dependent Schrödinger equation (TDSE) for two fermions and bosons in one and two dimensions (1D and 2D) (Refs. 15 and 16) and time-dependent Hartree-Fock (TDHF) results for $N=2-4$. We show that, in fact, there coexist *two independent breathing modes* one of which is λ dependent and the relative spectral weight of

which varies with λ. Further, fermions and bosons have the same breathing modes in 1D, whereas a substantial difference is observed in higher dimensions.

II. MODEL AND SOLUTION PROCEDURE

We start by considering two identical particles ($m_1 = m_2 \equiv m$, $q_1 = q_2 \equiv q$) in a harmonic potential of frequency Ω with Coulomb repulsion, described by the TDSE of two particles

$$\left[i\frac{\partial}{\partial t} + \frac{1}{2}\left(\frac{\partial^2}{\partial \mathbf{r}_1^2} + \frac{\partial^2}{\partial \mathbf{r}_2^2} \right) - V(\mathbf{r}_1, \mathbf{r}_2) \right] \Psi(\mathbf{r}_1, \mathbf{r}_2, t) = 0, \quad (1)$$

$$V = \frac{\mathbf{r}_1^2}{2} + \frac{\mathbf{r}_2^2}{2} + \frac{\lambda}{|\mathbf{r}_1 - \mathbf{r}_2|}, \quad (2)$$

where the total potential V is the sum of harmonic confinement and Coulomb repulsion. The coupling parameter—the ratio of the mean interaction and single-particle energy—is given by

$$\lambda = \frac{q^2}{4\pi\epsilon_0 l_0} \frac{1}{\hbar\Omega} \quad (3)$$

with the oscillator length $l_0 = \sqrt{\hbar/m\Omega}$. Throughout this work, lengths, times, and energies will be given in units of l_0, Ω^{-1} and $\hbar\Omega$, respectively.

A. Initial conditions

Equation (1) has to be supplemented by an initial condition for the two-particle wave function. Here we use either a symmetric (S) or antisymmetric (A) function, $\Psi_0^{S,A} = \Psi^{S,A}(\mathbf{r}_1, \mathbf{r}_2, 0) = \pm \Psi^{S,A}(\mathbf{r}_2, \mathbf{r}_1, 0)$, the symmetry of which is preserved during the time evolution since the Hamiltonian is spin independent. For the actual form of $\Psi_0^{S,A}$ we choose a stationary solution of Eq. (1) which is computed by imaginary time stepping. To single out time-dependent solutions of Eq. (1) of pure BM type we use two different excitation methods: (I) a fast switch of the trap frequency Ω and (II) the response to a periodic modulation of Ω.[17] While the former has computational advantages, the latter is more easily realized experimentally.[8]

B. Numerical solution of the TDSE

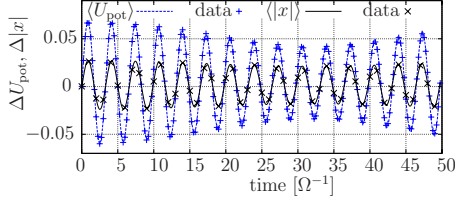We solve the two-particle TDSE (1) numerically using two independent methods: (i) a standard grid-based Crank-

FIG. 1. (Color online) Time evolution of the one-particle potential energy $\Delta U_{\text{pot}} = \langle U_{\text{pot}}\rangle(t) - U_{\text{pot},t=0}$ and $\Delta|x| = \langle|x|\rangle(t) - |x|_{t=0}$ for $N = 2$ particles in a 1D trap at $\lambda = 1.0$, obtained by solving Eq. (1), symbols. Lines: fit, Eq. (4), with frequencies $\omega_r = 1.901$ and $\omega_R = 2.0$.

Nicolson scheme (cn) with at least 1000 grid points in each direction and (ii) by expanding the wave function into a basis of oscillator eigenfunctions using up to $N_b = 625$ basis functions. The numerical parameters are adjusted for each value of λ, such that the results are fully converged with respect to the time-step size, the simulation box size and the number of grid points/basis functions. This has to be undertaken very carefully especially in the case of large λ, where the repulsive Coulomb interaction attains large values and the accurate numerical treatment becomes challenging.

III. RESULTS

A. Dynamics following a switch of the confinement

Let us start with an antisymmetric initial state Ψ_0^A and apply method (I). This is realized by turning off the trap for a short time, typically $\Delta t = 0.1 \ \Omega^{-1}$, after which it is restored (the explicit time dependence is not relevant as long as the excitation is spectrally much broader than Ω). During the "off" cycle, the Coulomb repulsion drives the particles out of their initial equilibrium state and initiates the BM.

To quantify the oscillatory motion we compute the time-dependent expectation value of the single-particle potential energy $\langle U_{\text{pot}}\rangle(t)$ with respect to the external trap and, independently, the expectation value $\langle|x|\rangle(t)$ which is directly associated with the monopole oscillation. Our numerical results confirm that both quantities exhibit identical time dependencies. In Fig. 1 we show the result for $N = 2$ in a 1D trap at an intermediate coupling, $\lambda = 1$, where we expect a quantum BM (QBM) with frequency in between the ideal quantum and classical limits, 2 and $\sqrt{3}$, respectively. However, the simulations reveal a different behavior with evidence of a beating of *two oscillations*. This is readily confirmed by applying a two-frequency fit

$$f(\omega_r, \omega_R, t) = a \cdot \sin[\omega_r(t - t_0)] + b \cdot \sin[\omega_R(t - t_0')] + f_0 \tag{4}$$

to our data (f stands for $\langle U_{\text{pot}}\rangle$ or $\langle|x|\rangle$), where t_0 and t_0' indicate phase shifts, a and b are the amplitudes, and ω_r and ω_R the frequencies of the two QBMs, and f_0 is the unperturbed (equilibrium) value of f. With the values $\omega_R = 2$ and $\omega_r = 1.901$ perfect agreement with the simulations is achieved, cf. lines in Fig. 1.

The origin of the two QBMs becomes immediately clear from the structure of Eq. (1). It can be solved with a product
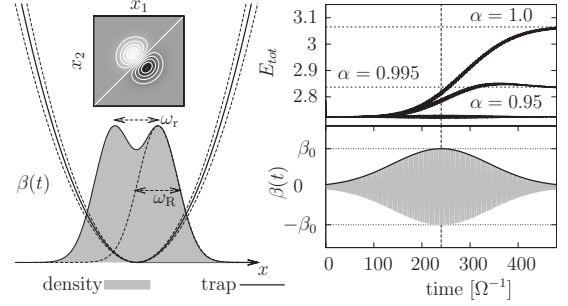

FIG. 2. Resonance excitation (II) for $\lambda = 1.0$ and three frequencies, $\omega_{\text{ext}} = \alpha\omega_r$ with $\alpha = 0.95, 0.995, 1.0$. Left: antisymmetric initial state (top) and particle density (gray area). Arrows indicate the two breathing motions. Right: time evolution of the total energy for the three external frequencies (top) and the exciting pulse (bottom).

ansatz, $\Psi(\mathbf{R}, \mathbf{r}, t) = \phi(\mathbf{R}, t) \cdot \varphi(\mathbf{r}, t)$, factorizing into functions of the center of mass (CoM) and relative coordinates, $\mathbf{R} = (\mathbf{r}_1 + \mathbf{r}_2)/2$, and $\mathbf{r} = \mathbf{r}_1 - \mathbf{r}_2$, resulting in two independent TD-SEs

$$i\partial_t \varphi(\mathbf{r}, t) = \left(-\frac{\partial^2}{\partial \mathbf{r}^2} + \frac{1}{4}\mathbf{r}^2 + \frac{\lambda}{r}\right)\varphi(\mathbf{r}, t), \tag{5}$$

whereas $\phi(\mathbf{R}, t)$ obeys a simple harmonic-oscillator problem which is independent of λ

$$i\partial_t \phi(\mathbf{R}, t) = \left(-\frac{1}{4}\frac{\partial^2}{\partial \mathbf{R}^2} + \mathbf{R}^2\right)\phi(\mathbf{R}, t). \tag{6}$$

This well-known splitting indicates the existence of two independent motions related to the relative and the CoM problem corresponding, in case of excitation (I), to two QBMs with the characteristic frequencies ω_r and ω_R, respectively. Obviously, Eq. (6) leads, in our case, to the (ideal) QBM with frequency $\omega_R = 2$ because it is just the TDSE for a single harmonic oscillator with mass $m = 2$, see Ref. 18. Thus, for all couplings λ, the system (1) possesses two QBMs, one with a universal frequency $\omega_R = 2$ and one with a λ-dependent frequency ω_r; the two modes are depicted by the arrows in the left part of Fig. 2, for an illustration, see Ref. 19. In the ideal quantum limit, $\lambda \rightarrow 0$, Eq. (5) transforms to Eq. (6) leading to a twofold degenerate mode with frequency ω_R.[20]

B. Resonance excitation. Absorption spectrum

We now verify these results by applying the resonance excitation (II), i.e., using a periodically modulated trapping potential of the form $\Omega^2[1 + \beta(t)]\mathbf{r}_i^2/2$, with $\beta(t) = \beta_0 \exp[-(t - t_0)^2/2\sigma]\sin(\omega_{\text{ext}}t)$ and $i = 1, 2$. Since we expect a strong resonance for $\omega_{\text{ext}} = \omega_r$ and $\omega_{\text{ext}} = \omega_R$ we use a small modulation depth and a finite pulse width, typically $\beta_0 = 5 \cdot 10^{-3}$, $t_0 = 240$, and $\sigma = 100$. The system response is characterized by the behavior of the total energy, E_{tot}, see Fig. 2 for typical examples. For a quantitative analysis we use the value E_{tot}^∞ sufficiently long after the excitation (cf. the dotted horizontal lines).

We now construct the absorption spectra by recording the values $E_{\text{tot}}^\infty(\omega_{\text{ext}}, \lambda)$, by scanning the frequency ω_{ext} for a
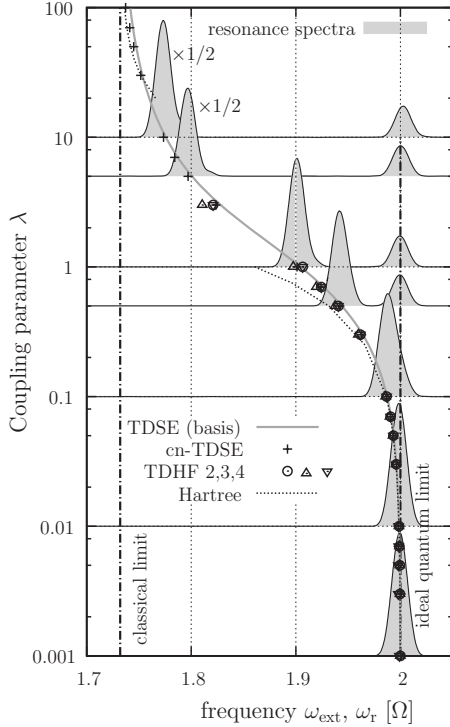
FIG. 3. QBM frequencies ω_r and ω_R for $N=2$ particles in a 1D trap versus λ from solution of Eq. (5) with a basis expansion method (gray line) and a cn solution of Eq. (1), (+) using excitation method (I). Grey resonance spectra (E_{tot}^∞) are the result of method (II). Dashed lines: classical ($\lambda > 30$) and quantum ($\lambda < 1$) mean-field models, symbols: TDHF results for $N=2,3,4$, which coincide for $\lambda \leq 1$.

given λ and repeating this procedure for a broad range of λ values. The resonance peaks are shown in Fig. 3 and confirm the existence of two frequencies. Their values fully agree with the result of method (I), cf. the gray line. Moreover, from the peak areas we can deduce the relative spectral weight of the two modes, clearly showing the continuous transition from the ideal quantum limit (where the mode ω_R dominates) to the strongly coupled classical case. Both peaks merge at weak coupling, around $\lambda=0.01$ (for the given σ). On the other hand, even for λ as large as 20, the pure quantum mode ω_R is clearly observable, being of the same absolute importance as for $\lambda=0$.

Furthermore, we underline that our approach of solving the full two-particle TDSE is applicable beyond the linear-response regime. It allows us to estimate the exact energy-absorption spectrum including the line shapes which obviously depend on the type of the external perturbation used. This is of special importance for experimental situations, where every excitation has finite duration and typical modulations which will also result in characteristic line shapes.

C. Analytical approximations for ω_r

In addition to the numerical results it is possible to derive semianalytical expressions for the breathing frequency ω_r in the two limits of weak and strong coupling, respectively. To obtain ω_r for small λ, we use a quantum-mechanical Hartree

model. Since for $\lambda \ll 1$, the interaction potential w is a small perturbation it can be approximated by the ansatz

$$w(\mathbf{r}_1 - \mathbf{r}_2) \approx \frac{1}{2} \sum_{i \neq j} \int d^3\mathbf{r}\, w(\mathbf{r}_i - \mathbf{r}) |\phi_j^{\lambda=0}(\mathbf{r})|^2 \quad (7)$$

involving the densities of the ideal (undisturbed) one-particle states. This potential, together with the external potential, gives rise to a renormalized confinement with the effective harmonic-trap frequency Ω^{eff} yielding the QBM frequency $\omega_r = 2\,\Omega^{\text{eff}}$. As can be seen in Fig. 3 the result is very close to the exact numerical solution of the TDSE for $\lambda \lesssim 0.3$, cf. the dotted line.

Similarly, for large λ, we construct a semiclassical mean-field theory, where the particles have a finite width and are modeled by Gaussian densities $n(x)$. For any λ the corresponding widths are taken from exact diagonalization calculations yielding $\omega_r = 1 + 2\lambda V''(|d_0|)$, with the mean-field potential

$$V(|d|) = \int dx_1 dx_2 \frac{n(x_1)n(x_2)}{x_1 - x_2 + |d|} \quad (8)$$

and the pertinent equilibrium distance d_0. Figure 3 shows that this approximation works well for $\lambda \gtrsim 30$ (dashed line).

One advantage of these approximations is that they can be straightforwardly extended to larger particle numbers. Yet the most interesting parameter range where quantum and correlation effects are strong simultaneously (around $\lambda=1$) are not accessible by perturbation approximations and require a full numerical treatment.

D. ω_r for more than two particles

Let us now discuss the dependence of ω_r on the number of particles N. In the case of classical charged particles in a harmonic trap it is well known that the breathing frequency is universal, i.e., ω_r does not depend on N. This case describes the limit of strong coupling, $\lambda \to \infty$. On the other hand, for the quantum case at finite λ, this question is still open. It turns out that a numerical solution of the full time-dependent N-particle Schrödinger equation for $N \geq 3$ with a sufficient accuracy is computationally very expensive. Therefore, we performed instead time-dependent Hartree-Fock calculations for three and four particles using a harmonic-oscillator representation of the HF equations,[21] see the symbols in Fig. 3. Full agreement with the TDSE results is observed for $N=2$, up to $\lambda \sim 3$. Further, the data for $N=3,4$ are very close to the TDSE results for $N=2$ up to $\lambda \sim 1$. From this we expect that also the exact $\omega_r(\lambda)$ is only very weakly N dependent as in the ideal quantum ($\lambda=0$) and classical limits.[13] However, a conclusive answer to this question requires a thorough computational analysis on the basis of the TDSE for larger particle numbers.

IV. INFLUENCE OF THE SPIN STATISTICS ON THE BREATHING MODE

A. One-dimensional system

Let us now repeat the above calculations with excitations (I) and (II), now starting from a symmetric initial-coordinate
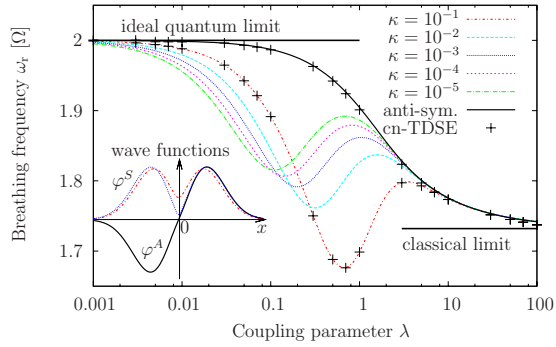
FIG. 4. (Color online) Frequency ω_r for two particles with a symmetric initial state in a 1D trap from numerical solution of the TDSE using a softened Coulomb potential. Crosses correspond to solution method (I) and lines to method (II), see Sec. II B. For $\kappa = 0$, ω_r is the same for symmetric and antisymmetric states. The result for the antisymmetric case is shown by the monotonic full (black) line. A finite κ drastically influences ω_r for the symmetric case which is explained by the behavior of the relative wave function at $x = 0$ (see inset).

wave function Ψ_0^S. According to the Bose-Fermi mapping in 1d (Ref. 22) it is expected, that both initial states, Ψ_0^S and Ψ_0^A, should lead to the same QBM. However, it is interesting to note that both numerical approaches to solve the TDSE (see Sec. II B) fail to reproduce this behavior due to the singularity of the Coulomb potential. The standard "regularization" procedure which introduces a small finite cut off κ in the potential, $\lambda/\sqrt{(x_1 - x_2)^2 + \kappa^2}$, yields qualitatively wrong results for ω_r, cf. Fig. 4. The breathing frequency ω_r exhibits a nonmonotonic dependence on λ, in contrast to the solution of the TDSE for an antisymmetric initial state. Reducing the cut-off parameter κ slightly improves the behavior by reducing the amplitude of the oscillation and shifting it toward smaller values of λ. But even for κ as small as 10^{-5} the spurious oscillation persists for $\lambda \lesssim 1$ and no convergence to the behavior of the antisymmetric state is observed.

We underline that this is not a numerical error and not due to the solution procedure but it is a property of the regularized Coulomb potential in 1D. The reason for the observed unexpected behavior is the incorrect (finite) value of the relative wave function φ_0^S at the origin (i.e., at zero particle separation). This reduces the particle repulsion and, thus, ω_r, cf. inset of Fig. 4.[23]

B. 2D and 3D systems

The situation changes completely in two and three dimensions. Now particles can avoid each other, allowing for finite values $\varphi_0^S(0)$, whereas $\varphi_0^A(0)$ remains equal to zero. Consequently, we expect a lowering of ω_r for symmetric states, compared to antisymmetric ones, for arbitrary λ. This is fully confirmed by numerical solutions of the TDSE,[24] cf. Fig. 5. The overall behavior is the same as in 1D—we observe a QBM with $\omega_R = 2$ and a second mode $\omega_r(\lambda)$, however, its value is different from 1D: the frequency is reduced (increased) for an (anti)symmetric state, cf. Fig. 5. While the differences vanish in the classical (and quantum) limits due
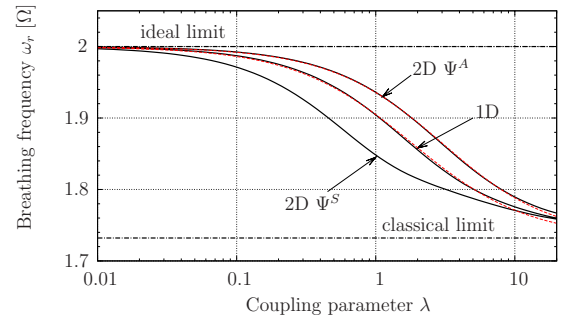

FIG. 5. (Color online) QBM frequency ω_r, for $N = 2$ in a 2D *trap* for symmetric and antisymmetric states from solution of the TDSE (Eq. (5)) with $\kappa = 0$. For comparison, also the 1D result and the two fits $w_r^{fit}(\lambda)$, Eq. (9), are shown by the (red) dotted lines.

to missing (complete) wave-function overlap, at intermediate couplings, around $\lambda = 1$, the differences between 1D and 2D, as well as between antisymmetric and symmetric states are substantial, reaching values of about 3% and 5%, respectively. These differences render the QBM frequency $\omega_r(\lambda)$ a sensitive diagnostics of the spin statistics of the particles. Indeed, in case of a symmetric spin-wave function (e.g., spin-polarized system in a strong magnetic field), the antisymmetric (symmetric) relative coordinate wave function φ_0 refers to fermions (bosons) and, vice versa, in case of an antisymmetric spin-wave function. Furthermore, in case of a mixture of fermions and bosons, the resonance absorption (II) yields information about the fraction of the different components.

While our results have been obtained for systems with a spin-independent Hamiltonian, it is straightforward to perform analogous TDSE calculations with spin effects included. Another interesting observation is that $\omega_r(\lambda)$ in 1D and 2D for the wave function φ_0^A is well described by the functional form

$$\omega_r^{fit}(\lambda) = a \exp[-\arctan(b\lambda + c)] + d,$$

$$\text{with} \quad d = (2 - \sqrt{3}d_c)/(1 - d_c),$$

$$d_c = \exp(\pi/2 - \arctan c),$$

$$a = (\sqrt{3} - d)\exp(\pi/2), \tag{9}$$

cf. Fig. 5.[25]

Finally, we expect that the reported collective behavior will be observable also in anisotropic harmonic traps in d dimensions with the difference that there will be a total of $2d$ QBMs with frequencies ω_R^i and $\omega_r^i(\lambda)$ where $i = 1, \ldots, d$.

V. SUMMARY AND DISCUSSION

In this paper we have presented a complete analysis of the quantum breathing modes of interacting charged particles in a 1D and 2D harmonic trap for arbitrary values of the coupling strength λ. The results are based on accurate solutions of the TDSE with two independent excitation scenarios and differ qualitatively from previous results based on hydrody-

namic models. We have shown that the frequency ratio $\gamma(\lambda)=\omega_r(\lambda)/\omega_R$, while being independent of the trap frequency and the confining system, does depend on the trap dimensionality and on fundamental properties of the particles: their spin statistics and the form of their pair interaction. Furthermore the λ dependence of γ is a sensitive measure of the strength of many-body effects in the particle ensemble.

The present results have been obtained for two particles with Coulomb interaction where exact solutions of the TDSE are possible. Nevertheless, they are representative for any nonideal quantum system in a harmonic trap. An analogous but different λ dependence exists for dipole interaction[15] and for short-range potentials. Thus, for a given value of λ, ω_r is indicative of the form of the pair interaction.

While our results are of importance for any nonideal quantum system in a harmonic trap, they are of particular relevance for electrons[2] and excitons[26] in quantum dots as well as for Bose and Fermi systems and their mixtures in traps or optical lattices. There the resonance absorption by the QBM, in particular, the relative spectral weight of the two modes, may serve as a valuable experimental diagnostics. Thereby one can take advantage of the comparatively easy excitation of the breathing mode using the excitation scenarios I or II.

At the same time the presented precise values of $\gamma(\lambda)$ provide a strong benchmark for nonequilibrium theoretical models and computational many-body methods for finite systems, including hydrodynamics, TDHF and time-dependent density-functional theory and nonequilibrium Green's functions.[21,27] Indeed, the normal modes of trapped systems are an important criterion for the quality of nonequilibrium

simulations which treat the interaction approximately. This is in complete analogy to approximate simulations of atoms which should reproduce the excitation energy spectrum as accurately as possible. Recently it was shown that the sloshing (Kohn) mode of a harmonically trapped system is preserved exactly by any conserving many-body approximation.[28] Similarly, the breathing mode may serve as such a constraint. For example, as was shown in Fig. 2, the time-dependent Hartree-Fock approximation behaves very well for an antisymmetric initial state (fermions). For symmetric states (bosons) Hartree-Fock simulations of strongly correlated charged systems in a harmonic trap have recently been developed[29] but the results for the breathing mode appear to be significantly less accurate than for fermions.

Finally, a particularly remarkable observation made in our paper is the persistence of the center-of-mass quantum breathing mode with frequency ω_R up to very large λ values. In strongly coupled systems this mode shows up in a "breathing" of *each individual particle* (see lower left part of Fig. 2 and the accompanying video[19]). Despite the fact that for strong coupling, the collective quantum degeneracy effects are weak (the interparticle distance is much smaller than l_0) each individual particle clearly "remembers" its quantum nature.

---

*bonitz@physik.uni-kiel.de

[1] F. Baletto and R. Ferrando, Rev. Mod. Phys. **77**, 371 (2005).

[2] A. V. Filinov, M. Bonitz, and Yu. E. Lozovik, Phys. Rev. Lett. **86**, 3851 (2001).

[3] A. V. Filinov, Yu. E. Lozovik, and M. Bonitz, Phys. Status Solidi B **221**, 231 (2000)

[4] S. M. Reimann and M. Manninen, Rev. Mod. Phys. **74**, 1283 (2002).

[5] I. Bloch, Nat. Phys. **1**, 23 (2005).

[6] S. Giorgini, L. P. Pitaevskii, and S. Stringari, Rev. Mod. Phys. **80**, 1215 (2008).

[7] A. Görlitz, J. M. Vogels, A. E. Leanhardt, C. Raman, T. L. Gustavson, J. R. Abo-Shaeer, A. P. Chikkatur, S. Gupta, S. Inouye, T. Rosenband, and W. Ketterle, Phys. Rev. Lett. **87**, 130402 (2001).

[8] H. Moritz, Th. Stöferle, M. Köhl, and T. Esslinger, Phys. Rev. Lett. **91**, 250402 (2003).

[9] C. Menotti and S. Stringari, Phys. Rev. A **66**, 043610 (2002).

[10] P. Pedri, S. De Palo, E. Orignac, R. Citro, and M. L. Chiofalo, Phys. Rev. A **77**, 015601 (2008).

[11] I. Bloch, J. Dalibard, and W. Zwerger, Rev. Mod. Phys. **80**, 885 (2008).

[12] A. Filinov, J. Böning, M. Bonitz, and Yu. Lozovik, Phys. Rev. B **77**, 214527 (2008).

[13] C. Henning, K. Fujioka, P. Ludwig, A. Piel, A. Melzer, and M. Bonitz, Phys. Rev. Lett. **101**, 045002 (2008).

[14] B. Partoens, and F. M. Peeters, J. Phys.: Condens. Matter **9**, 5383 (1997).

[15] $1d$ results for $l=3$ have been obtained in Ref. 10 within a hydrodynamical model, whereas for $l=2$, ω_{BM} is known to be λ independent (Ref. 16).

[16] M. R. Geller and G. Vignale, Phys. Rev. B **53**, 6979 (1996).

[17] We should note, that both excitations, (I) and (II), have vanishing dipole moments. Therefore, no dipole oscillation, as, e.g., the well-known Kohn mode, can be excited.

[18] Note that for other types of excitation other center-of-mass motions will be observed. In particular, a dipole excitation will give rise to the familiar sloshing or Kohn mode which is independent of N, dimensionality, interaction or quantum, and spin effects.

[19] See EPAPS Document No. E-PRBMDO-80-055929 for a video illustrating the oscillation behavior of two particles in 2D. For more information on EPAPS, see http://www.aip.org/pubservs/epaps.html.

[20] For $1/r^2$ interaction the existence of a twofold degenerate BM with $\omega_R=\omega_r=2$ was reported in Ref. 16.

[21] K. Balzer and M. Bonitz, J. Phys. A **42**, 214020 (2009).

[22] M. Girardeau, J. Math. Phys. **1**, 516 (1960).

[23] In contrast, φ_0^A vanishes at the singularity and the numerical result for ω_r is correct, in the limit of small κ. Hence, we used φ_0^A in our 1D calculations.

[24] In 2D, the Coulomb integrals converge and no cut-off parameter κ is required.

[25] The limits, $\omega_r(0)=2.0$ and $\omega_r(\lambda \rightarrow \infty)=\sqrt{3}$ are built in. In 1D (2D) the parameters are $b=0.867(b=0.204)$ and $c=1.742(c=0.296)$.

[26] A. Filinov, M. Bonitz, and Yu. E. Lozovik, J. Phys. A **36**, 5899 (2003); P. Ludwig, A. Filinov, Yu. Lozovik, H. Stolz, and M. Bonitz, Contrib. Plasma Phys. **47**, 335 (2007); A. Filinov, P. Ludwig, Yu. E. Lozovik, M. Bonitz, and H. Stolz, J. Phys.: Conf. Ser. **35**, 197 (2006); P. Ludwig, A. Filinov, M. Bonitz, and H. Stolz, Phys. Status Solidi B **243**, 2363 (2006).

[27] K. Balzer, M. Bonitz, R. van Leeuwen, A. Stan, and N. E. Dahlen, Phys. Rev. B **79**, 245306 (2009).

[28] M. Bonitz, K. Balzer, and R. van Leeuwen, Phys. Rev. B **76**, 045341 (2007).

[29] M. Heimsoth and M. Bonitz, Physica E (to be published).